Title
ESR ABSORPTION AND RELAXATION MECHANISM FOR p-BENZOSE-MIQUINONE IN THE ZEEMAN REGION

Author
Acrivos, J. V.

Publication Date
1962-08-01

UCRL-10133

University of California

Ernest O. Lawrence Radiation Laboratory

Berkeley, California

DISCLAIMER

Submitted for publication in Journal of Chemical Physics

UCRL-10133

UNIVERSITY OF CALIFORNIA

Lawrence Radiation Laboratory
Berkeley, California

Contract No. W-7405-eng-48

ESR ABSORPTION AND RELAXATION MECHANISM FOR p-BENZOSEMIQUINONE IN THE ZEEMAN REGION

J. V. Acrivos

August 1962

ESR Absorption and Relaxation Mechanism for p-Benzosemiquinone in the Zeeman Region

J. V. Acrivos

Inorganic Materials Research Division of the
Lawrence Radiation Laboratory, University of California
Berkeley, California

Abstract

The spin-lattice interaction for a free radical undergoing rapid Brownian motion, in the absence of electronic exchange, has been studied in the Zeeman region. The experimental and theoretical investigation indicates that the following relaxation mechanisms are all present in the case of the p-benzosemiquinone ion in sodium ethylate-ethanol solutions: (a) the intramolecular anisotropic hyperfine interaction, (b) the spin-orbit-phonon, Raman type, interaction, and (c) the modulation of the isotropic hyperfine energy of interaction by the electron distribution in the neighborhood of the free radical.

INTRODUCTION

The ESR absorption of the p-benzosemiquinone ion in sodium ethylate-ethanol has been studied in the field range of ±10 oe, in the temperature interval t=25° to -50°C, and at radio frequency energies less than the corresponding zero field hyperfine splittings, for the purpose of investigating the dominant relaxation mechanisms of this free radical. In this region, all the Zeeman transitions, including the hyperfine transitions, which had not been observed to this date by direct electromagnetic detection, have been completely resolved and identified.

The relaxation mechanisms for the different spin eigenstates of a paramagnetic ion undergoing rapid Brownian motion in solution is determined by the transitions that are induced by any or all of the following possible mechanisms: (a) the time dependent perturbation of inter and intramolecular anisotropic hyperfine interactions[1,2,3,4], (b) the spin-orbit coupling,[4,5,6,7] where the transitions induced by the anisotropy of the electronic g-factor[4,6] andd the spin-orbit-phonon interactions are special cases, and (c) the electronic[8] and chemical[9] exchange interactions where the latter introduce a modulation of the isotropic hyperfine coupling constant,[10,11] by disturbing the electron distribution in the neighborhood of the free radical.

Fraenkel et al.[4,12] investigated the relaxation mechanisms for the p-benzosemiquinone in the Paschen-Back region and concluded that case (a) above was the dominant process. However, in the Zeeman region it has been found that all three cases mentioned above significantly affect the lifetime of the Zeeman levels. Moreover, for free radical concentrations of the order of 10^{-3}M, the same line widths have been observed in high,[13,14] as well as in low fields, a fact which excludes the possibility of relaxation via the

anisotropy of the g-factor since, for this case, the line widths should be proportional to the square of the resonance frequency.

EXPERIMENTAL RESULTS

The ESR spectra of .001 to .006M p-benzoquinone in .04M $NaOC_2H_5$ in C_2H_5OH were determined with a Varian 4200 wide line spectrometer, at the constant frequencies: ν = 16.416; 16.217; 13.590 and 9.916 Mc/sec. The laboratory field, H, homogeneous to .01 oe within the volume of the sample, was sinusoidally modulated at a frequency ν_M=412 cps, with an amplitude of H_M=.02 oe and the spectra were recorded at the rate of $\left|\frac{dH}{dt}\right|$ = .01 oe./sec., in the range of ±10 oe. A fresh sample was prepared for each run and the free radical concentration was found to be constant throughout the recording time of a complete spectrum, as evidenced by the reproducibility of the intensity about zero field, shown in Fig. 1. The spectra in Fig. 1 are identified as those of the p-benzosemiquinone ion, at room temperature. The ESR absorption was studied in the interval t=25° to -50°C, where the temperature was measured to ±0.5°C by means of a copper-constantan thermocouple. The low temperature Dewar has been described elsewhere.[15] In addition to the proton hyperfine interaction at low temperatures, the ESR absorption indicates the existence of a hyperfine interaction with two sodium ions. This ESR absorption at t=-49.5°C is shown in Fig. 2 for the central proton hyperfine component.

ANALYSIS OF THE ESR SPECTRA

The ESR absorption obeys the selection rules:

$$|\Delta F| = 0 \text{ or } 1, \quad \Delta F^z = \pm 1, \qquad (1)$$

where at room temperature,

$$\vec{F} = \vec{S} + \sum_{i=1}^{4} \vec{I}_i \quad (S = \tfrac{1}{2},\ I_H = \tfrac{1}{2}) .$$

The steady state spin eigenfunctions of F^2 and F^2, transform within the D_{2h} group, according to the symmetry operations of the molecule ion where the irreducible representation is:

$$\Gamma = {}^2A_g + {}^1B_{1g} + {}^1B_{2u} + {}^1B_{3u} + 2\,{}^0A_g \,. \qquad (2)$$

The superscript gives the total nuclear spin angular momentum for the symmetry species.

The ESR spectra are analyzed according to the spin Hamiltonian:

$$\mathcal{H}^s = \left[|\gamma_e| S^z - \gamma_p \sum_{i=1} I_i^z \right] H + A \sum_{i=1}^{4} \underset{\sim}{I} \cdot \underset{\sim}{S} + \sum_n \sum_{i \neq j} J_n \underset{\sim}{I}_i \cdot \underset{\sim}{I}_j \,. \qquad (3)$$

$(n=o,m,p)$

$\gamma_e = g\beta$ and $\gamma_p = g_p\beta_0$ are the gyromagnetic ratios for the free electron and the proton respectively, where $|\beta|$ and β_0 are the Bohr and nuclear magneton. A and J_n, n=0, m, p, are the isotropic electron-proton, and proton-proton spin coupling constants for, respectively, ortho, meta and para protons.

The room temperature steady state spin eigenfunctions are given in Table 1 and the Breit-Rabi[16] energy levels are shown in Fig. 3. The nuclear hyperfine energy is not included in the Breit-Rabi levels, since, in this case, the levels of the same symmetry are shifted equally by the nuclear interaction, and therefore do not contribute to the ESR spectrum. Also, $J_n \approx 10$ cps[17] whereas A=6.6 Mc/sec.[12,13] at low temperatures the total quantum number is given by $\underset{\sim}{F}' = \underset{\sim}{F} + \sum_{i=1}^{2} \underset{\sim}{I}_{Na_i}$ and the steady state spin eigenfunctions are obtained from the reduced direct product of the eigenfunctions in Table 1 with those of the two sodium ions. The latter reduce in the C_2 symmetry group according to:

$$\Gamma = {}^3A + {}^2B + {}^1A + {}^0B \qquad (4)$$

Table 2 gives the spin eigenfunctions for the spin system 2 Na^{23}.

The theoretical ESR absorption spectra, shown in Fig. 1, were calculated according to the functional dependence of the resonance field given in Table 3. At t = -49.5°C the $(Na^{23})_2$ hyperfine splitting of the proton ^0A_g transitions, shown in Fig. 2, was calculated by making use of the spin eigenfunctions and energies given in Table 2 correct to second order in the sodium coupling constant with respect to the applied field. The measured coupling constants are:

$$A\,(e - H') = 6.631 \pm .003 \text{ Mc/sec.}$$

$$A'(e - Na^{23}) = 0.34 \pm .05 \text{ Mc/sec,}$$

The ESR absorption line widths between the points of maximum slope at 16.416 Mc/sec. are

a) for T = 298°K

$\Delta\nu_{ms} = 258 \pm 5$ kc/sec, for $^0A_g : |1/2,1/2\rangle \longleftrightarrow |1/2,-1/2\rangle$

$\langle \Delta\nu_{ms} \rangle = 297 \pm 40$ kc/sec, all others.

b) for T = 223.5°K

$\Delta\nu_{ms} = 150 \pm 15$ kc/sec.

for the $(Na^{23})_2$ proton hyperfine components of the ^0A_g transitions. The line widths were found to be independent of the initial concentration of the p-benzoquinone for concentrations below .005 M.

The hyperfine transitions which are observed when the rf energy is less than the zero field splitting, are of negative polarity with respect to the electronic transitions, since ΔF^z is of opposite sign, as shown by the Breit-Rabi energy levels in Fig. 3. This effect appears as a change in sign of the slope of the absorption derivative in Fig. 1. Also, in zero field, when $h\nu = 2.5|A|$ and $1.5|A|$, there will be theoretically no ESR absorption due to the fact that two identically probable transitions of opposite polarity are present. This is shown in Fig. 4 and 5.

Table 1. - Spin Functions of the p-Benzosemiquinone Ion in the D_{2h} Group

[a,b] Spin Function	Energy
^2A_g: $\lvert S, S^z \rangle$	
1. $\lvert 5/2,\ 5/2 \rangle = \alpha(a_g)_2$	$(\frac{1}{2} \lvert r_e \rvert -2r_p)H + A + \frac{1}{2}J$
2. $\lvert 3/2,\ 3/2 \rangle = \underset{\sim}{R}(\theta_3)\,\alpha(a_g)_1$	$-\frac{1}{2}r_pH - \frac{1}{4}A + \frac{1}{2}J + C_3$
3. $\lvert 5/2,\ 3/2 \rangle$ $\quad\quad\ \beta(a_g)_2$	$-\frac{3}{2}r_pH - \frac{1}{4}A + \frac{1}{2}J - C_3$
4. $\lvert 3/2,\ 1/2 \rangle = \underset{\sim}{R}(\theta_1)\,\alpha(a_g)_0^{g}$	$-\frac{1}{2}r_pH - \frac{1}{4}A + \frac{1}{2}J + C_1$
5. $\lvert 5/2,\ 1/2 \rangle$ $\quad\quad\ \beta(a_g)_1$	$-\frac{1}{2}r_pH - \frac{1}{4}A + \frac{1}{2}J - C_1$
6. $\lvert 3/2,-1/2 \rangle = \underset{\sim}{R}(\theta_{-1})\,\alpha(a_g)_{-1}$	$\frac{1}{2}r_pH - \frac{1}{4}A + \frac{1}{2}J + C_{-1}$
7. $\lvert 5/2,-1/2 \rangle$ $\quad\quad\ \beta(a_g)_0^{g}$	$\frac{1}{2}r_pH - \frac{1}{4}A + \frac{1}{2}J - C_{-1}$
8. $\lvert 3/2,-3/2 \rangle = \underset{\sim}{R}(\theta_{-3})\,\alpha(a_g)_{-2}$	$\frac{3}{2}r_pH - \frac{1}{4}A + \frac{1}{2}J + C_{-3}$
9. $\lvert 5/2,-3/2 \rangle$ $\quad\quad\ \beta(a_g)_{-1}$	$\frac{3}{2}r_pH - \frac{1}{4}A + \frac{1}{2}J - C_{-3}$
10. $\lvert 5/2,-5/2 \rangle = \beta(a_g)_{-2}$	$-(\frac{1}{2} \lvert r_e \rvert - 2r_p)H + A + \frac{1}{2}J$
^2A_g	
11. $\lvert 1/2,\ 1/2 \rangle_1 = \underset{\sim}{R}(\theta_0)\,\alpha(a_g)_0^{u_1}$	$\frac{1}{2}\lvert r_e \rvert H + \frac{1}{2}J + C_0$
12. $\lvert 1/2,\ 1/2 \rangle_2$ $\quad\quad\ \alpha(a_g)_0^{u_1}$	$\frac{1}{2}\lvert r_e \rvert H + \frac{1}{2}J - C_0$
13. $\lvert 1/2,-1/2 \rangle_1 = \underset{\sim}{R}(\theta_0)\,\beta(a_g)_0^{u_1}$	$-\frac{1}{2}\lvert r_e \rvert H + \frac{1}{2}J + C_0$
14. $\lvert 1/2,-1/2 \rangle_2$ $\quad\quad\ \beta(a_g)_0^{u_2}$	$-\frac{1}{2}\lvert r_e \rvert H + \frac{1}{2}J - C_0$

Table 1 - (continued)

$^{c}A_{1g}, {}^{1}B_{2u}, {}^{1}B_{3u}$

15.	$\|3/2, 3/2\rangle = \alpha(\Gamma)_1$, $(\Gamma = {}^{b}_{1g}, {}^{b}_{2u}, {}^{b}_{3u})$	$(\frac{1}{2}\|r_e\| - r_p)H + \frac{1}{2}A + K(\Gamma)$
16.	$\|1/2, 1/2\rangle = R(\theta'_1) \times \alpha(\Gamma)_0$	$-\frac{1}{2}r_pH - \frac{1}{4}A + K(\Gamma) + C'$
17.	$\|3/2, 1/2\rangle \quad \beta(\Gamma)_1$	$-\frac{1}{2}r_pH - \frac{1}{4}A + K(\Gamma) - C'_1$
18.	$\|1/2,-1/2\rangle = R(\theta_{-1}) \times \alpha(\Gamma)_{-1}$	$\frac{1}{2}r_pH - \frac{1}{4}A + K(\Gamma) + C'_1$
19.	$\|3/2,-1/2\rangle \quad \beta(\Gamma)_0$	$\frac{1}{2}r_pH - \frac{1}{4}A + K(\Gamma) - C'_1$
20.	$\|3/2,-3/2\rangle = \beta(\Gamma)_{-1}$	$-(\frac{1}{2}\|r_e\| - r_p)H + \frac{3}{2}A + K(\Gamma)$

---

a. The nuclear spin functions are expressed according to the species in the D_{2h} group from which they are generated, thus:

$$(\Gamma)_{I^z} = \frac{1}{g}\sum_P \chi^{\Gamma}(P)\, P\, |I^z\rangle$$

where P represents all the symmetry operations of the group, of dimension $g = 8$, and $\chi^{\Gamma}(P)$ are the corresponding characters for the species Γ. α and β are the spin eigenfunctions of S^2, S^z with $S = \frac{1}{2}$.

b. The $R(\theta)$ are the proper two dimensional rotation operators:

$$R(\theta_n) = \begin{pmatrix} \cos\theta_n & \sin\theta_n \\ -\sin\theta_n & \cos\theta_n \end{pmatrix}$$

where

for $n = 2^z$

$$\cos 2\theta_n = \frac{\Delta_n}{C_n}$$

$$\sin 2\theta_n = \frac{c_n A}{C_n}$$

for $n = 0$

$$\cos 2\theta_0 = \frac{\frac{1}{2}(3J_p - J)}{C_0}$$

$$\sin 2\theta_0 = \frac{\frac{3}{2}(J_0 - J_m)}{C_0}$$

$$\Delta_n = \frac{1}{2}\left[(|r_e| + r_p)H + \frac{n}{2}A\right]$$

$$J = J_0 + J_m + J_p$$

$$c_m = \frac{1}{2}\left[(I^2 + I^z)(I \pm I^z + 1)\right]^{1/2}$$

$$c_{\pm 3} = 1$$

$$c_{\pm 1} = \sqrt{\frac{3}{2}}$$

$$c'_{\pm 1} = \frac{1}{\sqrt{2}}$$

o $^1B_{1g}$, $^1B_{2u}$, $^1B_{3u}$ are degenerate, except for the nuclear spin coupling energy, thus:

$$K(^1B_{1g}) = J_p - \frac{1}{2} J$$

$$K(^1B_{2u}) = J_m - \frac{1}{2} J$$

$$K(^1B_{3u}) = J_o - \frac{1}{2} J$$

TABLE 3: Spin Eigenfunctions for the System $_{11}Na^{23}$ in the C_2 Group

[a] Spin Function: $|I,I^2>$

^3A :

1. $|3,3> = a\,a$
2. $|3,2> = 2^{-1/2}(ab+ba)$
3. $|3,1> = 5^{-1/2}(3^{1/2}bb+ab'+b'a)$
4. $|3,0> = 20^{-1/2}[aa'+a'a+3(bb'+b'b)]$
5. $|3,-1> = 5^{-1/2}[3^{1/2}b'b'+a'b+ba']$
6. $|3,-2> = 2^{-1/2}(a'b'+b'a')$
7. $|3,-3> = a'a'$

^1A :

1. $|1,1> = 10^{-1/2}[2bb-3^{1/2}(ab'+b'a)]$
2. $|1,0> = 20^{-1/2}[3(aa'+a'a)-(bb'+b'b)]$
3. $|1,-1> = 10^{-1/2}[2b'b'-3^{1/2}(a'b+ba')]$

^2B :

1. $|2,2> = 2^{-1/2}(ab-ba)$
2. $|2,1> = 2^{-1/2}(ab'-b'a)$
3. $|2,0> = 2^{-1/2}(aa'-a'a+bb'-b'b)$
4. $|2,-1> = 2^{-1/2}(a'b-ba')$
5. $|2,-2> = 2^{-1/2}(a'b'-b'a')$

^0B :

$|100> = 2^{-1}(aa'-a'a-bb'+b'b)$

[a] The spin eigenfunctions are given with respect to the value of the z component of angular momentum. Here a, b, b', a' correspond to $I^z_{Na} = 3/2,\ 1/2,\ -1/2,\ -3/2$, respectively.

Table 3: Transition Fields and Energies for the Zeeman Spectrum of the p-Benzosemiquinone Ion.

Allowed Transition	Resonance Field at Constant Frequency $(\|\gamma_e\| - \gamma_p) H$	[a] Relative Intensity I	Limits of the Transition Frequency: [b] Zero Field $\epsilon = h\nu$	I	Paschen-Back Region $\epsilon = h\nu$	I
^2A_g: $F^x = -\frac{5}{2} \rightarrow -\frac{3}{2}$						
1. $\Delta F=1$	$\pm \frac{\epsilon \pm 2.5A - \|\gamma_e\|\gamma_p \frac{H}{\epsilon}^2}{1 \pm .4977 \frac{A}{\epsilon}}$	$\cos^2\theta_{-3}$	-2.5A	5	$\|\gamma_e\|H_o$-2A	1
2. $\Delta F = 0$		$\sin^2\theta_{-3}$	0	0	-.5 A	0_1
$F^x = -\frac{3}{2} \rightarrow -\frac{1}{2}$ [c]						
3. $\Delta F=1$		$\cos^2\theta_{-3}\cos^2\theta_{-1}$	-2.5A	3	$\|\gamma_e\| H_o$-A	1
4. $\Delta F= -1$	$\pm 1.9970 \left\| \frac{A \pm \left[A^2 + (\epsilon^2 - \frac{25}{4}A^2)(1 - \frac{A^2}{4\epsilon^2})\right]^{\frac{1}{2}}}{(1 - \frac{A^2}{4\epsilon^2})} \right\|$	$\sin^2\theta_{-3}\sin^2\theta_{-1}$	2.5A	.5	-	0
5. $\Delta F = 0$		$\sin^2\theta_{-3}\cos^2\theta_{-1}$	0	0	.5A	[d] 0_1
6. $\Delta F=0$		$\cos^2\theta_{-3}\sin^2\theta_{-1}$	0	0	.5A	[d] 0_2

Table 3: (Continued)

Allowed Transition	Resonance Field at Constant Frequency $(\lvert\gamma_e\rvert - \gamma_p)H$	[a] Relative Intensity I	Limits of the Transition Frequency: Zero Field [b] $\epsilon = h\nu$	Zero Field I	Paschen-Back Region $\epsilon = h\nu$	Paschen-Back Region I
$F' = \frac{1}{2} \leftrightarrow \frac{1}{2}$	[c]					
7. $\Delta F = 1$		$\cos^2\theta_{-1}\cos^2\theta_1$	-2.5A	1.5	$\lvert\gamma_e\rvert H_o$	1
8. $\Delta F = -1$	$\pm 0.9970\left\{\frac{\epsilon^2 - \frac{25}{4}A^2}{1 - \frac{A^2}{4\epsilon^2}}\right\}^{\frac{1}{2}}$	$\sin^2\theta_{-1}\sin^2\theta_1$	2.5A	1.5	-	0
9. $\Delta F = 0$		$\sin^2\theta_{-1}\cos^2\theta_1$	0	0	.5A	[d] θ_2
10. $\Delta F = 0$		$\cos^2\theta_{-1}\sin^2\theta_1$	0	0	-.5A	[d] θ_2
$F' = \frac{1}{2} \leftrightarrow \frac{3}{2}$						
11. $\Delta F = 1$	[c]	$\cos^2\theta_1\cos^2\theta_3$	-2.5A	.5	$\lvert\gamma_e\rvert H_o + A$	1
12. $\Delta F = 1$	$\pm 0.9970\left\{\frac{-A \pm \left[A^2 + (\epsilon^2 - \frac{25}{4}A^2)(1 - \frac{A^2}{4\epsilon^2})\right]^{\frac{1}{2}}}{1 - \frac{A^2}{4\epsilon^2}}\right\}^{\frac{1}{2}}$	$\sin^2\theta_1\sin^2\theta_3$	2.5A	3	-	0
13. $\Delta F = 0$		$\sin^2\theta_1\cos^2\theta_3$	0	0	.5A	[d] θ_1
14. $\Delta F = 0$		$\cos^2\theta_1\sin^2\theta_3$	0	0	-.5A	[d] θ_2

Table 3: (Continued)

Allowed Transition	Resonance Field at Constant Frequency $(\lvert\gamma_e\rvert - \gamma_p)H$	[a] Relative Intensity I	Limits of the Transition Frequency [b] Zero Field e=hν	I	Paschen-Back Region e=hν	I
$F^2 = \frac{3}{2} \leftrightarrow \frac{5}{2}$						
15. $\Delta F = 0$	$\pm \frac{e \mp 2.5A - \lvert\gamma_e\rvert\gamma_p \frac{H^2}{e}}{1 \pm .4977 \frac{A}{e}}$	$\cos^2\theta_3$	0	0	$\lvert\gamma_e\rvert H_o + 2A$	1
16. $\Delta F = 1$		$\sin^2\theta_3$	2.5A	5	.5	[d] 0_1
$^0A_g: F^2 = -\frac{1}{2} \leftrightarrow \frac{1}{2}$						
17. $\Delta F = 0$	e	2	0	0	$\lvert\gamma_e\rvert H_o$	2
B_{1g}, B_{2u}, B_{3u}: $F^2 = -\frac{3}{2} \leftrightarrow -\frac{1}{2}$						
18. $\Delta F = 1$	$\pm \frac{e \pm 1.5A - \lvert\gamma_e\rvert\gamma_p \frac{H^2}{e}}{1 \pm .4977 \frac{A}{e}}$	$3\cos^2\theta'_{-1}$	-1.5A	4.5	$\lvert\gamma_e\rvert H_o - A$	3
19. $\Delta F = 0$		$3\sin^2\theta'_{-1}$	0	0	.5A	[d] $3\ 0_3$

Table 3: (Continued)

Allowed Transition	Resonance Field at Constant Frequency $(\lvert r_0 \rvert \mp r_p)H$	Relative Intensity[a] I	Limits of the Transition Frequency: Zero Field ε-hν	I	Paschen-Back Region ε-hν	I
$F^z = -\frac{1}{2} \leftrightarrow \frac{1}{2}$	[c]					
20. $\Delta F = 1$		$3 \cos^2\theta'_{-1} \cos^2\theta'_1$	-1.5A	1.5	$\lvert r_e \rvert H_o$	3
21. $\Delta F = -1$	$\pm .9970 \left\{ \frac{e^2 - \frac{9}{4}A^2}{1 - \frac{A^2}{4e^2}} \right\}^{\frac{1}{2}}$	$3 \sin^2\theta'_{-1} \sin^2\theta'_1$	1.5A	1.5	-	0
22. $\Delta F = 0$		$3 \sin^2\theta'_{-1} \cos^2\theta'_{-1}$	0	0	.5A	[d] $3\,0_3$
23. $\Delta F = 0$		$3 \cos^2\theta'_{-1} \sin^2\theta'_{-1}$	0	0	-.5A	[d] $3\,0_3$
$F^z = \frac{1}{2} \leftrightarrow \frac{3}{2}$						
24. $\Delta F = 0$	$\pm \frac{e \mp 1.5A - \lvert r_e \rvert r_p \frac{H^2}{e}}{1 \mp .4977 \frac{A}{e}}$	$3 \cos^2\theta'_1$	0	0	$\lvert r_e \rvert H_o + A$	3
25. $\Delta F = 1$		$3 \sin^2\theta'_1$	1.5A	4.5	.5A	[d] $3\,0_3$

Table 5: (Continued)

(a) The energy is doubly degenerate in H, and here the intensity is to be assigned according to the limiting value of ϵ when H=0.

(b) The transitions have been assigned assuming A is negative. If A were positive, although the line assignments would be incorrect, the features of the spectrum remain unchanged.

(c) In order to correct for the gyromagnetic ratio of the proton, ϵ is to be replaced by $\epsilon - \gamma_p H$.

(d) The hyperfine transitions in high fields are of a relative intensity:

$$O_1 = \frac{17}{4}\left(\frac{A}{H}\right)^2 + 4\left(\frac{\gamma_p}{\gamma_e}\right)^2$$

$$O_2 = \frac{13}{4}\left(\frac{A}{H}\right)^2 + 6\left(\frac{\gamma_p}{\gamma_e}\right)^2$$

$$O_3 = \frac{5}{4}\left(\frac{A}{H}\right)^2 + 6\left(\frac{\gamma_p}{\gamma_e}\right)^2$$

Relaxation Mechanisms

The fact that the linewidths observed in low as well as in high fields are of the same magnitude excludes the possibility of a relaxation mechanism through the anisotropy of the g-factor which predicts that the linewidths should be proportional to the square of the free electron Larmor precession frequency. Hence, at the dilutions used, the possible relaxation mechanisms should proceed through the inter and intramolecular anisotropic hyperfine interactions, through the spin-orbit interactions and through the time dependent variations of the isotropic hyperfine coupling constant. These processes, thus determine the steady state population subject to the conditions:

$$\dot{N}_k = \sum_j N_j W_{jk} - N_k \sum_j W_{kj} = 0, \quad (k=1, 2 \ldots n)$$

or

$$\underset{\sim}{W} \cdot \underset{\sim}{N} = 0 \tag{5}$$

where $\underset{\sim}{W}$ is the lattice and radiation field induced transition probability matrix and $\underset{\sim}{N}$ is the population distribution vector, with components N_k equal to the population of the state k. The room temperature transition probability matrix $\underset{\sim}{W}$ is factored according to the symmetry of the spin states as follows:

$$\underset{\sim}{W} \cdot \underset{\sim}{N} = \begin{pmatrix} \underset{\sim}{W}(^2A_g) & & & & & \\ & \underset{\sim}{W}(^0A_g) & & & & \\ & & \underset{\sim}{W}(^1B_{1g}) & & & \\ & & & \underset{\sim}{W}(^1B_{2u}) & & \\ & & & & \underset{\sim}{W}(^1B_{3u}) & \end{pmatrix} \cdot \underset{\sim}{N} = 0 \tag{6}$$

where the normalization conditions are:

$$\frac{1}{N} \sum_{(k \text{ in } {}^2A_g)} N_k = \frac{5}{16}$$

$$\frac{1}{N} \sum_{(k \text{ in } {}^0A_g)} N_k = \frac{2}{16}$$

$$\frac{1}{N}\sum_{(k \text{ in } {}^1B_{1g})} N_k = \frac{1}{N}\sum_{(k \text{ in } {}^1B_{2u})} N_k = \frac{1}{N}\sum_{(k \text{ in } {}^1B_{3u})} N_k = \frac{3}{15}$$

and

$$N = \sum_k N_k$$

The saturation parameter[4,18] for a given state will thus depend on the symmetry species:

$$S^{\Gamma}_{kj}(H_1) = \frac{N_k - N_j}{N^0_k - N^0_j} = (\Gamma = {}^2A_g,\ {}^0A_g,\ {}^1B_{1g},\ {}^1B_{2u},\ {}^1B_{3u}) \qquad (7)$$

where N^0_k and N_k are the respective populations of the state k for a Boltzmann distribution and in the presence of an rf field which induces transitions between the states j and k.

Absolute saturation experiments cannot be performed at room temperature since the free radical concentration does not remain constant for long periods of time. However, the differential saturation of the transitions ${}^0A_g|1/2, 1/2> \longleftrightarrow |1/2, -1/2>$ with respect to the rest indicates that the former saturate faster than the latter. Table 4 gives the observed relative intensities at room temperature, at $\nu = 16.416$ Mc./sec., and at two different power levels. These measurements were carried out by reducing the rf power progressively until the relative areas underneath the absorption curves were in agreement with the theoretically predicted intensities for all the transitions. It was not possible to saturate completely the ${}^0A_g$ transitions with respect to the others as all the hyperfine components were homogeneously broadened with increasing rf power.

The differential saturation can be explained according to the BPP[1,4] theory of anisotropic hyperfine interactions and the modulation of the isotropic hyperfine interaction by the time dependent perturbation of the electron

Table 4: Saturation of the ESR absorption of the p-Benzosemiquinone Ion at ν = 16.416 Mc/sec.

Transition	Relative Intensity of the Transition $^{0}A_{g}\|1\ 2,\ 1\ 2> \longleftrightarrow \|1\ 2,-1\ 2>$		
	Theoretical	Experimental (a) low rf power	Experimental (a) power increase by 10dB
$^{2}A_{g}: \|5/2,\ 3/2> \rightarrow \|5/2 \rightarrow 5/2>$	2.23	2.1 ± .1	1.8 ± .1
$B_{1g}, B_{2u}, B_{3u}: \|3/2,1/2> \rightarrow \|3/2,3/2>$	.68	.73 ± .05	.55 ± .05
[b] $B_{1g}, B_{2u}, B_{3u}: \|1/2,-1/2> \rightarrow \|5/2,3/2>$ $^{2}A_{g}: \|3/2,1/2> \rightarrow \|5/2,3/2>$	.68	.64 ± .05	.52 ± .05
$B_{1g}, B_{2u}, B_{3u}: \|1/2,1/2> \rightarrow \|3/2,\ 3/2>$	.70	.76 ± .05	.62 ± .05

(a) The experimental intensities are the averages for the observed spectra about zero field.

(b) At this frequency there is an accidental degeneracy of two transitions.

distribution in the neighborhood of the free radical,[11] neither of which influences the lifetime of the states of $^{5}A_{g}$ symmetry. These will be influenced only by perturbations independent of the proton nuclear spin quantum number such as the spin-orbit-phonon interactions.[7]

In the general formulation, the lattice induced transition probabilities are obtained from the Master equation:[1,19,20]

$$W^{0}_{jk} = \sum_{\ell} \frac{2\ \tau_{c\ell}}{1 + \omega_{jk}^{2}\tau_{c\ell}^{2}} \ < k|\mathcal{H}_{1\ell}(t)|\ k > ^{2} \qquad (8)$$

where $\mathcal{H}_{1\ell}(t)$ is the time dependent perturbation which causes the lattice to exchange energy with the spin states, $\tau_{c\ell}$ is the correlation time of the perturbation, and $\hbar\omega_{jk}$ is the energy separation between the states j and k. Hence the processes under investigation contribute to Eq. 8 as follows:

(a) The intramolecular anisotropic hyperfine interaction with respect to the axis of quantization, in the direction of the applied field, gives rise to a random time dependent perturbation with a correlation time given by the Debye[1,21] theory so that $\tau_{ca} \approx 1.1 \times 10^{-10}$ sec. When the p-benzosemiquinone ion is approximated by a sphere of radius = 3.4 A,[22] in alcohol at room temperature, with a viscosity $\eta = 0.011$ poise; at t = 50°C, $\eta = .0687$ and $\tau_{ca} \approx 6 \times 10^{-10}$ sec. The contribution to Eq. 8 is:

$$|< j\ |\mathcal{H}_{1,a}(t)\ | k >|^{2} = I_{I}(I_{I}+1)\ \mathcal{F}_{a}^{2} \cdot |\ < F_{j}F^{z}_{j}\ |\ \sum_{i,m} A^{m}_{2i}\ |F_{k}F^{z}_{k}>|^{2} \qquad (9)$$

where $\mathcal{F}_{a}^{2} = \frac{3}{5}\sum_{m=-2}^{2} |< \frac{1}{r_{i}^{3}}\ Y_{2,m}\ (\theta\phi)_{i} >|^{2}$

$$A^{0}_{21} = \frac{2}{3} I^{z}_{i}\, S^{z} - \frac{1}{6}\left(I^{+}_{i} S^{-} + I^{-}_{i} S^{+}\right)$$

$$A^{1}_{2i} = \frac{1}{\sqrt{6}}\left(I^{z}_{i} S^{+} + I^{+}_{i} S^{z}\right), \qquad A^{-1}_{21} = (A^{1}_{21})^{*}$$

$$A^{2}_{2i} = \frac{1}{\sqrt{6}} I^{+}_{i} S^{+}, \qquad A^{-2}_{21} = (A^{2}_{21})^{*}$$

$(r,\theta,\phi)_i$ are the spherical polar coordinates of the vector connecting the two interacting spins with respect to a molecular axis, and $Y_{2,m}$ are the associated spherical harmonics of order 2. Using Sidman's[23] SCF π - MO's together with the integrals in $_a$ evaluated by McConnell and Strathdee,[4,24] the contributions to Eq. (8) at ω = 16 Mc/sec. are:

$$W_{jk} \sim 4 \text{ to } 24 \times 10^4 \cdot I_\Gamma(I_\Gamma + 1) \cdot |< F_j F_j^z | \sum_{m,i} A_{2i}^m | F_k F_k^z >|^2 \qquad (10)$$

where the limits correspond to t=25° and -50°C, respectively. I_Γ is the total nuclear spin quantum number for the symmetry species Γ. The matrix elements of $< |A_{2i}^m| >$ for the spin eigenfunctions given in Table 1 are presented in Table 5.

Table 5: Matrix Elements of the Anisotropic Hyperfine Interaction

^2A_g	$\|5/2,5/2\rangle$	$\|5/2,3/2\rangle$	$\|5/2,1/2\rangle$	$\|5/2,-1/2\rangle$	$\|5/2,-3/2\rangle$	$\|5/2,-5/2\rangle$	$\|3/2,3/2\rangle$	$\|3/2,1/2\rangle$	$\|3/2,-1/2\rangle$	$\|3/2,-3/2\rangle$
$\|5/2,5/2\rangle$		$b\ c_1(3)$	$\frac{2}{3}\cos^2\theta_1$	0	0	0	$c_1(3+\frac{\Gamma}{2})$	$\frac{2}{3}\sin^2\theta_1$	0	0
$\|5/2,3/2\rangle$	$2/3$ as $E_+ =$ as $E_+ 0,1.6/3$		$c_2(3,1)$	$a^2\theta_3 c^2\theta_1$	0	0	$a\ A_1(3)$	$c_2(3,1+\frac{\Gamma}{2})$	$a^2\theta_3 c^2\theta_{-1}$	0
$\|5/2,1/2\rangle$	$2/3$ $.8/3$	$1/6$ $.64/3$		$\frac{1}{4}c^2(\theta_1+\theta_{-1})$	$a^2\theta_1 c^2\theta_3$	0	$c_2(3+\frac{\Gamma}{2},1)$	$A_2(1)$	$\frac{1}{8}a^2(\theta_1+\theta_{-1})$	$a^2\theta_1 c^2\theta_{-3}$
$\|5/2,-1/2\rangle$	0	0 $.48$	$.25$ 0		$c_2(-3+\frac{\Gamma}{2},-1+\frac{\Gamma}{2})$	$\frac{2}{3}\sin^2\theta_{-1}$	$a^2\theta_3 c^2\theta_{-1}$	$\frac{1}{8}a^2(\theta_1+\theta_{-1})$	$A_2(-1+\frac{\Gamma}{2})$	$c_2(-3+\frac{\Gamma}{2},-1+\frac{\Gamma}{2})$
$\|5/2,-3/2\rangle$	0	0	0 $.48$	$.25$ $.8/3$		$c_1(-3+3\frac{\Gamma}{2})$	0	$a^2\theta_1 c^2\theta_{-3}$	$c_2(-3+\frac{\Gamma}{2},-1+\frac{\Gamma}{2})$	$A_1(-3+\frac{\Gamma}{2})$
$\|5/2,-5/2\rangle$	0	0	0	0 $.8/3$	$1/6$ $1.6/3$		0	0	$\frac{2}{3}\cos^2\theta_{-1}$	$c_1(-3+\Gamma)$
$\|3/2,3/2\rangle$	$1/6$ $.3$	$1/9$ $.36$	$1/6$ $.27$	1 $.12$	0	0		$c_2(3+\frac{\Gamma}{2},1+\frac{\Gamma}{2})$	$a^2\theta_3 c^2\theta_{-1}$	0
$\|3/2,1/2\rangle$	0 $.4$	0 $.08$	$1/6$ $.06$	0 $.25$	1 $.32$	0	$.25$ $.08$		$\frac{1}{4}c^2(\theta_1+\theta_{-1})$	$c^2\theta_1 c^2\theta_{-3}$
$\|3/2,-1/2\rangle$	0	0 $.32$	0 $.25$	$1/6$ $.06$	$1/6$ $.02$	$2/3$ $.4$	0 $.04$	$.25$ 0		$c_2(-3,-1)$
$\|3/2,-3/2\rangle$	0	0	0 $.12$	0 $.27$	$1/9$ $.36$	$2/3$ $.3$	0	0 $.04$	$1/6$ $.08$	

Table 5: (continued)

(a) $^1B_{1g}, ^1B_{2u}, ^1B_{3u}$	$\|3/2,3/2>$	$\|3/2,1/2>$	$\|3/2,-1/2>$	$\|3/2,-3/2>$	$\|1/2,1/2>$	$\|1/2,-1/2>$
$\|3/2,3/2>$		$C_1'(1')$	$\cos^2\theta_{-1}'$	0	$C_1'(1'+\frac{\pi}{2})$	$\sin^2\theta_{-1}'$
$\|3/2,1/2>$	$\frac{1}{6}\frac{(1+\sqrt{3})^2}{16}$		$\frac{d}{4}c^2(\theta_1'+\theta_{-1}')$	$\sin^2\theta_1'$	$A_2(1')$	$\frac{1}{4}c^2(\theta_1'+\theta_{-1}')$
$\|3/2,-1/2>$	1 / 2/3	.25 / 0		$C_1'(-1'+\frac{\pi}{2})$	$\frac{1}{4}c^2(\theta_1'+\theta_{-1}')$	$A_2(1'+\frac{\pi}{2})$
$\|3/2,-3/2>$	0	0 / 2/3	.25 $\frac{(1+\sqrt{3})^2}{16}$		$\cos^2\theta_1'$	$C_1'(-1'+\pi)$
$\|1/2,1/2>$	.25 $\frac{(1-\sqrt{3})^2}{16}$	1/6 / .06	0 / .25	1 / 1/3		$\frac{1}{4}c^2(\theta_1'+\theta_{-1}')$
$\|1/2,-1/2>$	0 / 1/3	0 / .25	1/6 / .06	1/6 $\frac{(1-\sqrt{3})^2}{16}$	.25 / 0	

^0A_g	$\|1/2,1/2>_1$	$\|1/2,-1/2>_2$	$\|1/2,1/2>_2$	$\|1/2,-1/2>_2$
$\|1/2,1/2>_1$		0	$\frac{1}{48}\cos^2 2\theta_0$	0
$\|1/2,-1/2>_1$	0		0	$\frac{1}{48}\cos^2 2\theta_0$
$\|1/2,1/2>_2$	$\frac{1}{48}\cos^2 2\theta_0$	0		0
$\|1/2,-1/2>_2$	0	$\frac{1}{48}\cos^2 2\theta_0$	0	

(a) The proton-proton anisotropic hyperfine interaction has been neglected with respect to the electron-proton terms.

(b) According to the spin eigenfunctions given in Table 1,

$$C_1(i) = \frac{2}{3}\left[\cos\theta_i - \frac{1}{2}\sin\theta_i\right]^2$$

$$C_2(i,j) = \frac{1}{6}\left[\cos\theta_i\cos\theta_j + \sin\theta_i\cos\theta_j - \sqrt{\frac{3}{2}}\sin\theta_i\sin\theta_j\right]^2$$

$$A_1(i) = \left[\frac{\sin 2\theta_i}{2} + \frac{\cos 2\theta_i}{3}\right]^2$$

$$A_2(i) = \left[\frac{\sin 2\theta_i}{6} + \frac{\cos 2\theta_i}{\sqrt{6}}\right]^2$$

$$C_1(r) = \frac{1}{6}\left[\cos\theta_i - \sqrt{\frac{3}{2}}\sin\theta_i\right]^2$$

(c) The elements given below the diagonal are the limiting values of the transition probability in the Paschen-Back region and in zero field.

(d) For brevity, s and c correspond to the sine and cosine functions.

(e) The transition probabilities are obtained by multiplying each element by: $(\frac{h\pi}{5})\, g_n^2\beta_0^2\, \frac{1}{r_{pp}^6}$, where r_{pp} is the distance between the interacting protons.

Hence, according to Table 5, the states ^2A_g, $^1B_{1g}$, $^1B_{2u}$, and $^1B_{3u}$ may exchange energy with the lattice through intramolecular anisotropic electron-proton and proton-proton spin hyperfine interactions. However, the intramolecular anisotropic hyperfine operator induces transitions in the state ^3A_g only through proton-proton spin interactions, which are less probable than the electron-proton transitions by the factor:

$$\left[\gamma_p < \frac{1}{r_{p-p}^3} > \right]^2 \left[\gamma_e < \frac{1}{r_i^3} > \right]^{-2}$$

This effect leads to a maximum broadening of the state ^3A_g of $2C_o \approx 10$ cps,[15] which is negligible.

At the dilutions used, one free radical ion/3. x $10^5 A^3$, the intermolecular electron-electron spin anisotropic interaction are two orders of magnitude smaller than the intramolecular proton-electron spin interactions and therefore may be neglected with respect to the latter. The intermolecular electron-proton interactions with the solvent molecules may also be neglected.[4]

(b) The spin-orbit-phonon interactions provide a relaxation mechanism[5,7,18] which is independent of the nuclear spin quantum number. Indeed, the departure of the spectroscopic splitting factor, g = 2.0048,[13,14] from the free electron value, g_s = 2.0023,[25] indicates that the spin-orbit interaction has prevented a complete quenching of the orbital angular momentum by the crystalline electric field.[26] This mechanism, thus, must account for the lifetime of the ^2A_g spin states.

The spin-orbit interactions is:[27]

$$\mathcal{H}_{l,b} = \mathcal{H}_{SO} = \beta^2 [-i \text{ grad } V \cdot \underline{p} + 2 \underline{S} \cdot \text{grad } V \times \underline{p}] \qquad (11)$$

$\underline{p}$ is the linear momentum of the unpaired electron, of spin $S = \frac{1}{2}$ which moves in the Coulomb field of all the nuclei in the free radical ion plus all the surrounding molecules and ions. $V = -\sum_k Z_k/\rho_k$, where Z_k is the effective change of the k^{th} species above, at a ρ_k distance from the unpaired electron. The first term in $_{SO}$ is zero for non s-electrons in spherically symmetric fields, but for aromatic hydrocarbons in solution, where V is of lower symmetry,[28,29,30] it vanishes when the second term is non zero. Hence, in this case, for a field V of any symmetry:

$$\mathcal{H}_{SO} = -\mathcal{H}^*_{SO} = \sum_k \sum_{\zeta = (\rho,\theta,\phi)_k} (\lambda_\zeta \underline{L}_\zeta)_k \cdot \underline{S} \qquad (12)$$

where

$$\lambda_\rho = -i\beta^2 \frac{1}{\rho}\frac{\partial V}{\partial \rho};\ \lambda_\theta = -i\beta^2 \frac{1}{\rho^2}\frac{\partial V}{\partial \theta};\ \lambda_\phi = -i\beta^2 \frac{1}{\rho^2 \sin\theta}\frac{\partial V}{\partial \phi}$$

$$L_\rho^z = -i\frac{\partial}{\partial \phi};\ L_\theta^z = -i\cot\theta\frac{\partial}{\partial \phi};\ L_\phi^z = i\left(\rho\sin\theta\frac{\partial}{\partial \rho} + \cos\theta\frac{\partial}{\partial \theta}\right)$$

$$L_\rho^+ = e^{i\phi}\left(\frac{\partial}{\partial \theta} + \cot\theta\frac{\partial}{\partial \phi}\right);\ L_\theta^+ = -e^{i\phi}\left(\rho\frac{\partial}{\partial \rho} + i\frac{\partial}{\partial \phi}\right);\ L_\phi^+ = i e^{i\phi}\left(\sin\theta\frac{\partial}{\partial \theta} - \rho\cos\theta\frac{\partial}{\partial \rho}\right)$$

$L_\rho^- = -L_\rho^{+*}$, etc.

$(\rho,\theta,\phi)_k$ are the spherical polar coordinates of the unpaired electron with respect to the k^{th} species and a molecular axis of symmetry.

The spin-orbit interaction contributes to the value of the spectroscopic splitting factor as follows: In p-benzoquinone, $n \longleftrightarrow \pi^*$ singlet-triplet and singlet-singlet transitions have been observed at 2.3 and 2.7 ev., respectively.[31,32] For the free radical, the wave functions for the ground and excited states are:

$$|\Psi_o,\ S^z = \tfrac{1}{2}\rangle = \mathcal{A}\left\{\sum\prod (n)^2 (n')^2 \pi\right\}$$

$$|\Psi_{n\pi^*},\ S^z = \tfrac{1}{2}\rangle = \mathcal{A}\left\{\sum\prod 2^{-\frac{1}{2}}\left[(n)^2 n' \pi n(n')^2\right](\pi)^2\right] \qquad (13)$$

where $\mathcal{A}$ is the antisymmetrization operator and $\sum$ and $\prod$ represent the closed sigma and pi electron configurations. n and n' are the non-bonding orbitals localized at each oxygen atom, and π is the lcao mo occupied by the unpaired electron in the ground state. Also, due to the b_{2g} symmetry of π in the D_{2h} group, only $\Psi_{n\pi^*}$ contributes to the spin-orbit interaction. Hence, from the expression for the spectroscopic splitting factor in solution:

$$\langle g\rangle = g_e\left[1 - \frac{2}{3}\sum_{j=x,y,z}\sum_{k,m}\sum_{\zeta=(\rho,\theta,\phi)_k} \langle \lambda_\zeta L_\zeta^{j*}\rangle_{01}\langle L^j\rangle_{10}/(E_1 - E_0)\right], \qquad (14)$$

where o and 1 designate the ground and excited states , separated in energy by $E_1 - E_o$, the contribution from the n, π interaction is:

$$\langle \phi \rangle_{n,\pi} = g_s = [4\lambda_{co}\, \rho_o^{\pi}/3\Delta] \qquad (15)$$

where λ_{co} is the spin-orbit interaction term, which may be evaluated according to Eq. (12):

$$\lambda_{co} = \lambda_o - 2\beta^2 \left[R^{-3}\int_o^R Z_c |\mathcal{R}|^2 \rho^2\, d\rho + \int_R^{\infty} Z_c |\mathcal{R}|^2 \rho^{-1}\, d\rho\right] + \text{lattice terms} \qquad (16)$$

$\lambda_o = -152\ cm^{-1}$ is the spin orbit coupling constant for the oxygen atom, whereas the asymmetric term, due to the neighboring carbon atom at a bond distance $R = 1.30A$,[22] is only $-1\ cm^{-1}$ for a Slater 2p radial wave function, $\mathcal{R}$, which justifies the use of the spherically symmetric potential approximation to evaluate the g-factor.[26] The lattice terms are also negligible. ρ_o^{π} is the unpaired electron density at the oxygen atom, which can be evaluated from the splitting $\delta = 2\rho^{\pi} K$ between the singlet-triplet and singlet-singlet transitions for the neutral molecule where K is the exchange integral between orthogonal oxygen 2p atomic orbitals. For $K = .905$ ev,[33] $\rho_o^{\pi} = .221$. Δ is equal to the average of the above $n \longleftrightarrow \pi$ transitions, corrected for the difference in two center Coulomb integrals for the free radical and neutral molecule. Thus:

$$\Delta = 2.5\ ev + \left\langle \frac{1}{r_{12}}, (\pi_1)^2 (\pi_2)^2 \right\rangle - \left\langle \frac{1}{r_{12}}, (\pi_1)^2 (n_2)^2 \right\rangle \qquad (17)$$
$$\simeq 2.9\ ev.$$

The two center integrals were evaluated making use of the SCF - π MO's obtained by Sidman[23] for p-benzoquinone. This leads to $\langle g \rangle_{inc} = 2.0043$, and if one assumes that the contribution from the ring spin-orbit interactions is the same as for aromatic hydrocarbon negative ions, where $\langle \bar{g} \rangle = 2.0027$,[34] then the calculated g value is in agreement with the observed quantity, $g = 2.0048 \pm .0001$.[12,13,34]

The spin-orbit-phonon coupling between the states j and k is, thus:

$$\langle j|\mathcal{H}_{1,b}|k\rangle = \mathcal{F}_{jb}\cdot|\langle F_j F_j^z|\underline{S}|F_k F_k^z\rangle|^2 \qquad (18)$$

where correct to third order approximation:

$$\mathcal{F}_{jb} = \sum_i \left[\frac{\langle\mathcal{H}_{SO}\rangle_{ji}\langle\mathcal{H}_{OL}\rangle_{ik}}{E_j - E_i} + \frac{\langle\mathcal{H}_{OL}\rangle_{ji}\langle\mathcal{H}_{SO}\rangle_{ik}}{E_j - E_i}\right]$$

$$+\sum_{i,i'}\left[\frac{\langle\mathcal{H}_{SO}\rangle_{ji}\langle\mathcal{H}_{OL}\rangle_{ii'}\langle\mathcal{H}_{OL}\rangle_{i'k}}{(E_j - E_i)(E_j - E_{i'})} + \text{all possible permutation terms}\right].$$

The $|\langle|\underline{S}|\rangle|^2$ matrix elements, presented in Table 6, are independent of the nuclear spin quantum number and were evaluated from the corresponding eigenfunctions in Table 1. The second order terms in $\mathcal{F}_{jb}$ correspond to Zeeman interactions which are balanced by the emission or absorption of a phonon by the lattice. These processes are, therefore, proportional to the square of the resonance frequency and may be neglected according to the experimental evidence. The third order terms are of importance because they define the Raman mechanisms by which a spin transition at a frequency ω_o is balanced by the emission of a photon and the absorption of another at the respective frequencies ω and ω', in such a manner that $\omega - \omega' = \omega_o$, where ω takes all the possible values $\omega_o \leq \omega \leq \Omega$ so that the transition probability does not depend on the value of the resonance frequency. Ω is an upper cut off frequency characteristic of the system. An order of magnitude estimate of the contribution of the Raman processes to Eq. (8) is carried out as follows:

$$\langle\mathcal{H}^m_{SO}\rangle_{o,n_-} \cong \left(\frac{8\pi}{5}\frac{\hbar}{\rho\omega_o}\right)^{1/2}\cdot\lambda_{co}\cdot Y_{1,m}(\theta,\varphi),\ (m=0,\pm1)$$

$$\langle\mathcal{H}_{OL}\rangle_{i,i'} \cong \sum_j \frac{\partial V}{\partial q_j}\cdot Q_j\rangle_{i,i'} + \text{higher order terms},\ (i,i' = 0,n_-,n_+) \qquad (19)$$

Table 6: Matrix Elements of the Spin-Orbit Interactions: $\langle \Psi | \hat{R} | \Psi \rangle$

^0A_g	$\|5/2,5/2\rangle$	$\|5/2,3/2\rangle$	$\|5/2,1/2\rangle$	$\|5/2,-1/2\rangle$	$\|5/2,-3/2\rangle$	$\|5/2,-5/2\rangle$	$\|3/2,3/2\rangle$	$\|3/2,1/2\rangle$	$\|3/2,-1/2\rangle$	$\|3/2,-3/2\rangle$
$\|5/2,5/2\rangle$		$\frac{1}{4}\cos^2\theta_3$	0	0	0	0	$\frac{1}{4}\sin^2\theta_3$	0	0	0
$\|5/2,3/2\rangle$	.25 as $H\to\infty$ as $H\to 0$, .05		$\frac{1}{4}s^2\theta_3 c^2\theta_1$	0	0	0	$\frac{1}{4}\sin^2 2\theta_3$	$\frac{1}{4}s^2\theta_3 s^2\theta_1$	0	0
$\|5/2,1/2\rangle$	0	0 .08		$\frac{1}{4}s^2\theta_1 c^2\theta_{-1}$	0	0	$\frac{1}{4}c^2\theta_1 c^2\theta_3$	$\frac{1}{4}\sin^2 2\theta_1$	$\frac{1}{4}s^2\theta_1 s^2\theta_{-1}$	0
$\|5/2,-1/2\rangle$	0	0	0 .09		$\frac{1}{4}s^2\theta_{-1} c^2\theta_{-3}$	0	0	$\frac{1}{4}c^2\theta_{-1} c^2\theta_1$	$\frac{1}{4}\sin^2 2\theta_{-1}$	$\frac{1}{4}s^2\theta_{-1} s^2\theta_{-3}$
$\|5/2,-3/2\rangle$	0	0	0	0 .08		$\frac{1}{4}\sin^2\theta_{-3}$	0	0	$\frac{1}{4}c^2\theta_{-3} c^2\theta_{-1}$	$\frac{1}{4}\sin^2 2\theta_{-3}$
$\|5/2,-5/2\rangle$	0	0	0	0	0 .05		0	0	0	$\frac{1}{4}\cos^2\theta_{-3}$
$\|3/2,3/2\rangle$	0 .20	0 .16	.25 .04	0	0	0		$\frac{1}{4}c^2\theta_3 s^2\theta_1$	0	0
$\|3/2,1/2\rangle$	0	0 .12	0 .24	.25 .06	0	0	0 .03		$\frac{1}{4}c^2\theta_{-1} s^2\theta_{-1}$	0
$\|3/2,-1/2\rangle$	0	0	0 .12	0 .24	.25 .12	0	0	0 .04		$\frac{1}{4}c^2\theta_{-1} s^2\theta_{-3}$
$\|3/2,-3/2\rangle$	0	0	0	0 .04	0 .16	.25 .20	0	0	0 .03	

Table 6: (continued)

$B_{1g}, {}^1B_{2u}, {}^1B_{3u}$	$\|3/2,3/2>$	$\|3/2,1/2>$	$\|3/2,-1/2>$	$\|3/2,-3/2>$	$\|1/2,1/2>$	$\|1/2,-1/2>$
$\|3/2,3/2>$		$\frac{1}{4}\cos^2\theta_1'$	0	0	$\frac{1}{4}\sin^2\theta_1'$	0
$\|3/2,1/2>$	.25 1/12		$\frac{1}{4}s^2\theta_1'c^2\theta_{-1}'$	0	$\frac{1}{4}\sin^2 2\theta_1'$	$\frac{1}{4}s^2\theta_1's^2\theta_{-1}'$
$\|3/2,-1/2>$	0	0 1/9		$\frac{1}{4}\sin^2\theta_{-1}'$	$\frac{1}{4}c^2\theta_{-1}'c^2\theta_1'$	$\frac{1}{4}\sin^2 2\theta_{-1}'$
$\|3/2,-3/2>$	0	0	0 1/12		0	$\frac{1}{4}\cos^2\theta_{-1}'$
$\|1/2,1/2>$	0 1/6	0 2/9	.25 1/18	0		$\frac{1}{4}s^2\theta_{-1}'c^2\theta_1'$
$\|1/2,-1/2>$	0	0 1/18	0 2/9	.25 1/6	0 1/36	

${}^0A_g$	$\|1/2,1/2>_1$	$\|1/2,-1/2>_1$	$\|1/2,1/2>_2$	$\|1/2,-1/2>_2$
$\|1/2,1/2>_1$		.25	0	0
$\|1/2,-1/2>_1$	.25		0	0
$\|1/2,1/2>_2$	0	0		.25
$\|1/2,-1/2>_2$	0	0	.25	

where

$$V \cong -\sum_{i,k} \frac{Z_k}{R_{ik}} \sum_{\ell,m} \frac{4\pi}{2\ell+1} \left(\frac{r_i}{R_{ik}}\right)^{\ell} Y_{\ell,m}(\theta,\phi)_i \; Y^{*}_{\ell,m}(\beta,\gamma)_{ki}, \; (R_{ki} \geq r_i)$$

and the states in Eq. (13) are indicated by the subscript. (β,γ), $(R,\beta,\gamma)_{ki}$ and $(r,\theta,\phi)_i$ are, respectively, the spherical polar coordinates of the axis of symmetry parallel to the CO bond with respect to the applied field, and of the point charge Z_k and the unpaired electron with respect to the i^{th} atom and the axis of symmetry. $Y_{\ell,m}$ are the associated spherical harmonics of order ℓ, and Q_j are the normal coordinates. In particular, the significant contributions to $\langle \mathcal{H}_{OL} \rangle$ must arise from the stresses on the CO bond, so that the transition probability between two spin states is[17]

$$W_{jk,b} \sim \frac{(172.8)^2}{105} \pi^5 \cdot \left(\frac{kT}{mv^2}\right)^2 \cdot \left(\frac{\rho_o^{\pi} \lambda_{CO}}{\Delta^3}\right)^2 \cdot \left(\epsilon Z_c^2 \cdot \frac{\langle r^2 \rangle_{pp} \langle r \rangle_{pd}}{R^5}\right)^2 \cdot \Omega \cdot |\langle j|\xi|k \rangle|^2 \qquad (20)$$

where an isotropic distribution of the density of modes was assumed,[20,35] and $\Delta \geq kT \gg \omega,\omega' \gg \omega_o$. v is the velocity of sound in the system of mass m, $\langle r^2 \rangle_{pp}$ and $\langle r \rangle_{pd}$ are the radial integrals for an oxygen atom electron of the given symmetries and the non zero contribution is obtained by attributing a $3d_{xz}$ character, $\epsilon \approx 10^{-3}$ to 10^{-4}, to the nonbonding oxygen orbital which may be introduced by the bending of the CO bonds on collision. Hence, the transition probability for this system is,

$$W_{jk,b} \sim \left(\frac{T}{298}\right)^2 \cdot |\langle j|\xi|k \rangle|^2 \times 10^6 \text{ sec}^{-1} \qquad (21)$$

when $\langle r^2 \rangle_{pp} = 30/Z_o$ and $\langle r \rangle_{pd} = 4.75/Z_o$ for Slater type orbitals, $R = 2.46\ a_o$, $m \sim 16$, $v \sim 1.24 \times 10^5$ cm./sec. for the velocity of sound in ethanol at room temperature,[36] and $\Omega \sim 5 \times 10^{13}$ sec.$^{-1}$ for the characteristic frequency for the CO symmetric stretching mode.[37]

In the absence of chemical exchange, the validity of this mechanism can be tested for the temperature square law dependence of the line widths, in the region where the other parameters remain constant. These experiments, however, should be carried out in aprotic solvents,[38] where the motional effects,[8,20] introduced by the isotropic hyperfine interactions with the solvent molecules and ions, does not affect the line widths in the temperature interval studied. Nevertheless, the ESR absorption line widths for the ^6A_g transitions at T = 298°K and its $(Mn^{23})_2$ hyperfine components at T = 223.5°K do obey the square law dependence, where

$$\left(\frac{T}{T'}\right)^2 : \left(\frac{\Delta \nu_{ms}(T')}{\Delta \nu_{ms}(T)}\right) = 1.0 \pm .1 \qquad (22)$$

(c) In dilute solutions, where the electronic exchange is negligible, the random time dependent perturbation introduced by the electron density distribution in the neighborhood of the free radical will influence the lifetime of the Zeeman hyperfine levels of the same total symmetry and total component of angular momentum through the isotropic hyperfine interaction.[10,11] The completely orthonormalized unpaired electron wave function is :[39]

$$\phi_e = \left[\phi_o - \sum_{k \neq o} \langle \phi_k, \phi_o \rangle \phi_k \right] \left[1 - \sum_{k \neq o} | \langle \phi_k, \phi_o \rangle |^2 \right]^{-1/2} . \qquad (23)$$

where ϕ_o is the SCF wave function for the isolated free radical, and the Schmidt orthogonalization insures that the Pauli Principle is obeyed where the overlap integral $\langle \phi_o, \phi_k \rangle$ is non zero. $\{\phi_k\}$ is the orthonormal set which describes the surrounding molecules and ions. The electron density, correct to second order in the overlap integral is thus:

$$\rho = \left[\rho_{oo} - \sum_{k \neq o} \rho_{ok} \langle \phi_k, \phi_o \rangle + \sum_{k,k' \neq o} \rho_{kk'} \langle \phi_k, \phi_o \rangle \langle \phi_o, \phi_{k'} \rangle \right] \left[1 - \sum_{k \neq o} | \langle \phi_k, \phi_o \rangle |^2 \right]^{-1} . \quad (2$$

where $\rho_{\beta m} = \rho_{m\beta} \equiv |\phi^*_\beta \phi_m|$. Hence, for a system undergoing rapid Brownian motions, the isotropic hyperfine energy of interaction with a nucleus of spin I_p is modulated by the time dependence of the electron density distribution as follows:

$$\mathcal{H}_{hfs} = \left[A_o + A(t) \right] \vec{I} \cdot \vec{S} \qquad (25)$$

where

$$A_o \cong \delta_n \left[\rho_{oo} + \sum_{k \neq o} (\rho_{oo} + \rho_{kk}) |< \phi_k, \phi_o >|^2 \right]_{at\ \vec{r}_p}$$

$$A(t) \cong -\delta_p \left\{ \sum_{k \neq o} \rho_{ok} < \phi_k, \phi_o > \left[1 + \sum_{k \neq o} |< \phi_o, \phi_k >|^2 \right] \right\}_{at\ \vec{r}_p} \left(\delta_p = \frac{8\pi}{3} g \beta_p |\beta|\phi_o \right)$$

The contribution to Eq. (8) is thus:

$$W_{j,k,c} = \frac{2\tau_c}{1+\omega^2 \tau_c^2} \cdot I_p(I_p+1) \cdot < |\mathcal{F}_c|^2 > \cdot |< F_j | F_j^z \sum_i \vec{I}_i \cdot \vec{S} | F_k F^z >|^2 \qquad (26)$$

where

$F_j - F_k = \pm 1$; $\Delta M_I = 0$

$$< |\mathcal{F}_c|^2 > \cong \delta_p^2 \left[< |\sum_k \rho_{ok} < \phi_k, \phi_o > |^2 > \right]_{at\ \vec{r}_p}$$

$$= A_o \left[\sum_k \delta_p |\phi_k|^2 |< \phi_o, \phi_k >|^2 \right]_{at\ \vec{r}_p} \left(b = \frac{2\mu}{3} g \beta_p |\phi_o|^2 \right)$$

$$|< j | \sum_i \vec{I}_i \cdot \vec{S} | k >|^2 = \left(\frac{(I^- I^z)(I^+ I^z + 1)}{\hbar^2 (1 + F^z \frac{A_o}{H_o})^2 + (I^- I^z)(I^+ I^z + 1) \left(\frac{A_o}{H_o} \right)^2} \right)_r$$

The correlation time is a function of the dissociation of the complex formed by the free radical and the two sodium ions, $Q(Na)_2^+$:

$$Q(Na)_2^+ \underset{V_{-1}}{\overset{V_1}{\rightleftharpoons}} Q^- + 2Na^+ \qquad (27)$$

where at room temperature the rate constant for the dissociation reaction is greater than the coupling constant, $A^{\frac{1}{2}} = 3.4 \times 10^5$ sec.$^{-1}$. For a solution with [Q] = .006 M, the ESR absorption line broadening ensues at T = 270° to 275°K, which indicates that at room temperatub $\tau_{cc} \leq 1.7 \times 10^{-9}$ sec., when an Arrhenius law dependence is assumed for the rate constant. Since the hyperfine splitting in aprotic[39] and ionic, solutions are known for this free radical, $\langle |\mathcal{F}_c|^2 \rangle$ can be evaluated semiempirically, so that from Eq. (25) and (26):

$$\langle |\mathcal{F}_c|^2 \rangle \geq |A_o \cdot \delta A| \qquad (28)$$

where $A_o = -2.419$ oe.[38] is the proton hyperfine splitting in an aprotic solution and $\delta A = |A| - |A_o| = -.051$ oe. Hence,

$$W_{jk,c} \approx \frac{1.4\, c_n^2 \times 10^5\, I_T(I_T+1)}{\left(1+\Gamma^2 \frac{A}{\hbar}\right)^2 + 4\, c_n^2 \left(\frac{A}{\hbar}\right)^2} \text{ sec.}^{-1} \qquad (29)$$

is of the same order of magnitude as the transition probability given by the other mechanisms considered above. However, according to Eq. (29), W_c vanishes in zero fields, so that only mechanism (a) and (b) can contribute to the line width of the hyperfine transitions.

CONCLUSIONS

The transition probability between the Zeeman levels of the p-benzosemiquinone ion has been found to be of the same order of magnitude, $W \sim 10^5$ sec.$^{-1}$, for the three mechanisms under study, but only the spin-orbit-phonon interactions contribute to the lifetime of the proton ^2A_g hyperfine states. Hence these

transitions should, and indeed they do saturate faster than the rest. However, the predicted line width variation between the different hyperfine components, except for the $^{o}A_{g}$ transitions was not detected within the experimental uncertainty limits.

ACKNOWLEDGMENTS

The author wishes to thank Professors K.S. Pitzer, L. Brewer and A. Acrivos for encouragement and valuable criticism. This work was conducted under the auspices of the U.S.Atomic Energy Comission.

References

1. N. Bloembergen, E. M. Purcell and R. V. Pound, Phys. Rev. 73, 679 (1948).
2. R. Kubo and K. Tomita, J. Phys. Soc. Japan 9, 888 (1954).
3. D. Kivelson, J. Chem. Phys. 27, 1087 (1957); 33, 1094 (1960).
4. M. Stephen and G. K. Fraenkel, J. Chem. Phys. 32, 1435 (1960).
5. A. Landesman, J. Phys. Rad. 20, 937 (1959).
6. H. M. McConnell, J. Chem. Phys. 25, 709 (1956); 34, 13 (1961).
7. J. H. Van Vleck, Phys. Rev. 57, 429 (1939).
8. P. W. Anderson, and P. R. Weiss, Rev. of Mod. Phys. 25, 269 (1953).
9. H. S. Gutowsky, D. W. McCall and C. P. Slichter, J. Chem. Phys. 21, 279 (1953).
10. H. M. McConnell and A. D. McLachlan, J. Chem. Phys. 34, 1 (1961).
11. J. V. Acrivos, submitted for publication to the J. Chem. Phys.
12. J. W. H. Schreus, G. E. Blomgren and G. K. Fraenkel, J. Chem Phys. 32, 1861 (1960).
13. J. L. Vivo, PhD Thesis, University of Minnesota (1956).
14. B. Venkataraman, B. C. Segal and G. K. Fraenkel, J. Chem. Phys. 30, 1006 (1959).
15. J. V. Acrivos and K. S. Pitzer, J. Phys. Chem. (in press).
16. G. Breit and C. I. Rabi, Phys. Rev. 38, 2082 (1931).
17. J. A. Pople, W. G. Schneider and H. J. Bernstein, "High Resolution Nuclear Magnetic Resonance" McGraw-Hill (1959) p. 193.
18. J. P. Lloyd and G. E. Pake, Phys. Rev. 94, 579 (1954).
19. Y. Ayant, J. Phys. et Rad. 16, 411 (1955).
20. A. Abrayam, "The Principles of Nuclear Magnetism," Oxford, (1961) Ch. 8 and 9.
21. P. Debye, "Polar Molecules," Dover Publications, Inc., New York, 1945, Ch. V.
22. H. J. M. Bowen, J. Donohue, D. G. Jenkin, O. Kennard, P. J. Wheatley, and D. H. Whiffen, "Interatomic Distances," London Chem. Society, 1958; M194.

23. J. W. Sidman, J. Chem. Phys. 27, 429 (1957), Table II.

24. H. M. McConnell and J. Strathdee, J. Mol. Phys. 2, 129 (1959).

25. J. E. Nafe and E. Nelson, Phys. Rev. 75, 1194 (1949).

26. H. M. McConnell and R. E. Robertson, J. Phys. Chem. 61, 1018 (1957).

27. L. I. Schiff, "Quantum Mechanics," McGraw-Hill Book Co., New York, 1955, p. 352.

28. M. Mizushima and S. Koide, J. Chem. Phys. 20, 765 (1952).

29. E. Clementi and M. Kasha, J. Mol. Spectroscopy 2, 297 (1958).

30. D. S. McClure, J. Chem. Phys. 20, 682 (1952).

31. H. M. McConnell, J. Chem. Phys. 20, 700 (1952).

32. J. W. Sidman, J. Am. Chem. Soc. 78, 2363 (1956).

33. J. M. Parks and R. Parr, J. Chem. Phys. 32, 1657 (1960), Table X.

34. M. S. Blois, Jr., H. W. Brown and J. E. Maling, Bull. Ampere, 9^{e} annee, fasc. special, 243, (1960).

35. R. E. Peirls, "Quantum Theory of Solids," Clorendor Press, Oxford Press, Oxford, (1955).

36. "Handbook of Chemistry and Physics," Chemical Rubber publishing Co., Cleveland, Ohio (1959), p. 2500.

37. G. Herzberg, "Molecular Structure and Molecular Spectra," Vol. II., D. Van Nostrand Co., Inc. New York (1954), p. 195.

38. A. H. Maki and D. H. Geske, J. Chem. Phys. 33, 825 (1960); E. W. Stone and A. H. Maki, ibid 36, 1944 (1962).

39. [illegible]

40. B. S. Gourary and F. J. Adrian, Phys. Rev. 105, 1180, (1957).

List of Figures

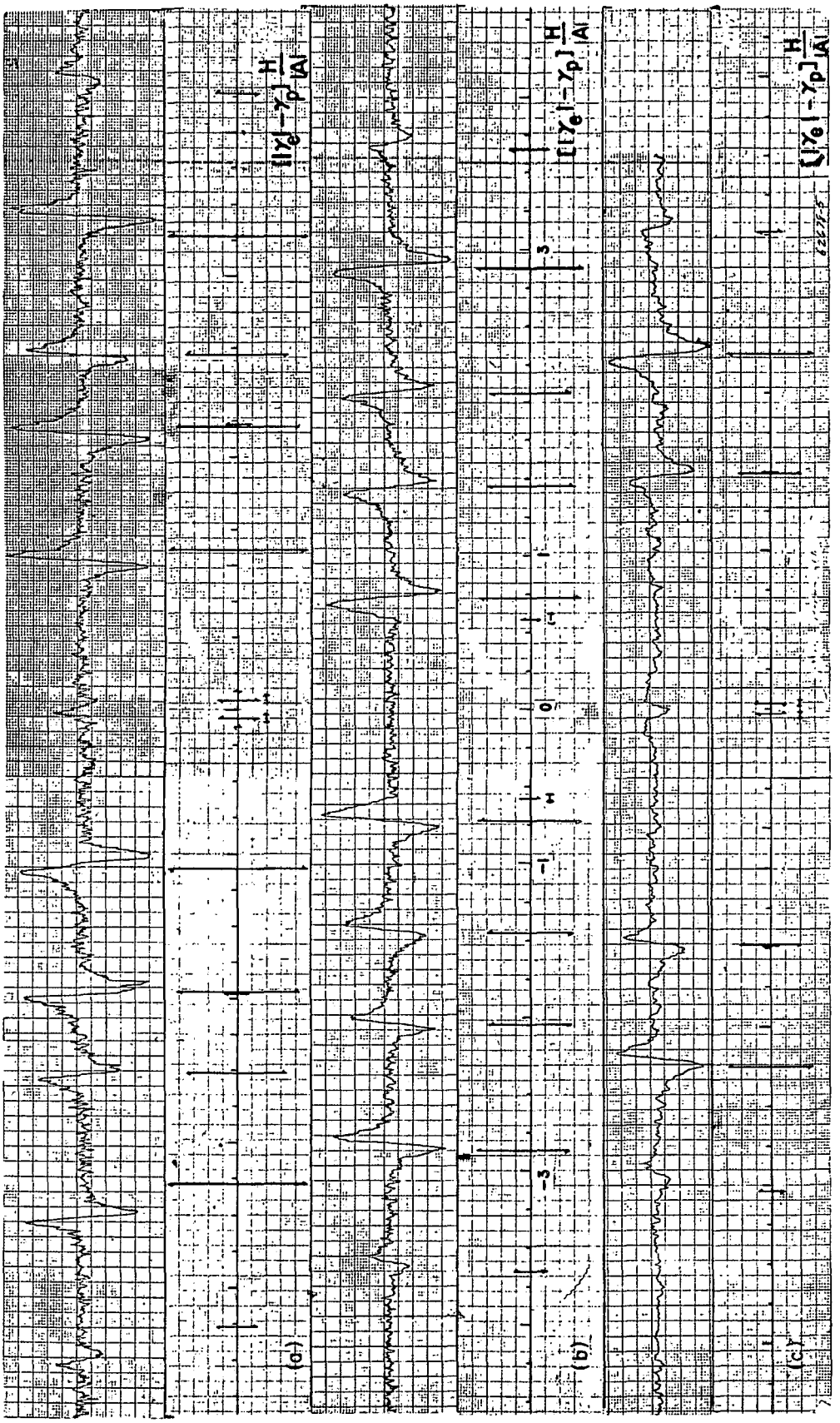

Fig. 1

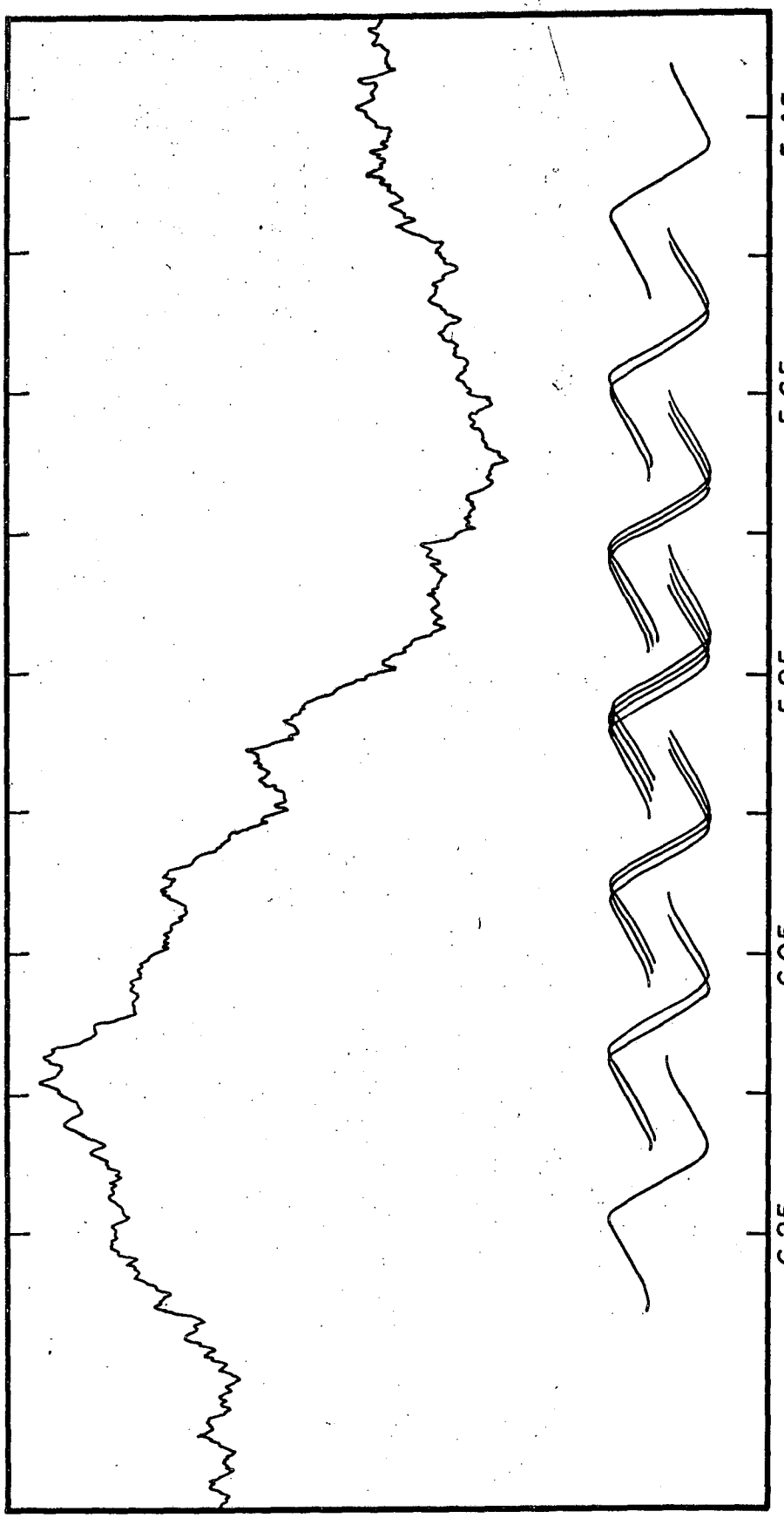

MU-27570

Fig. 2

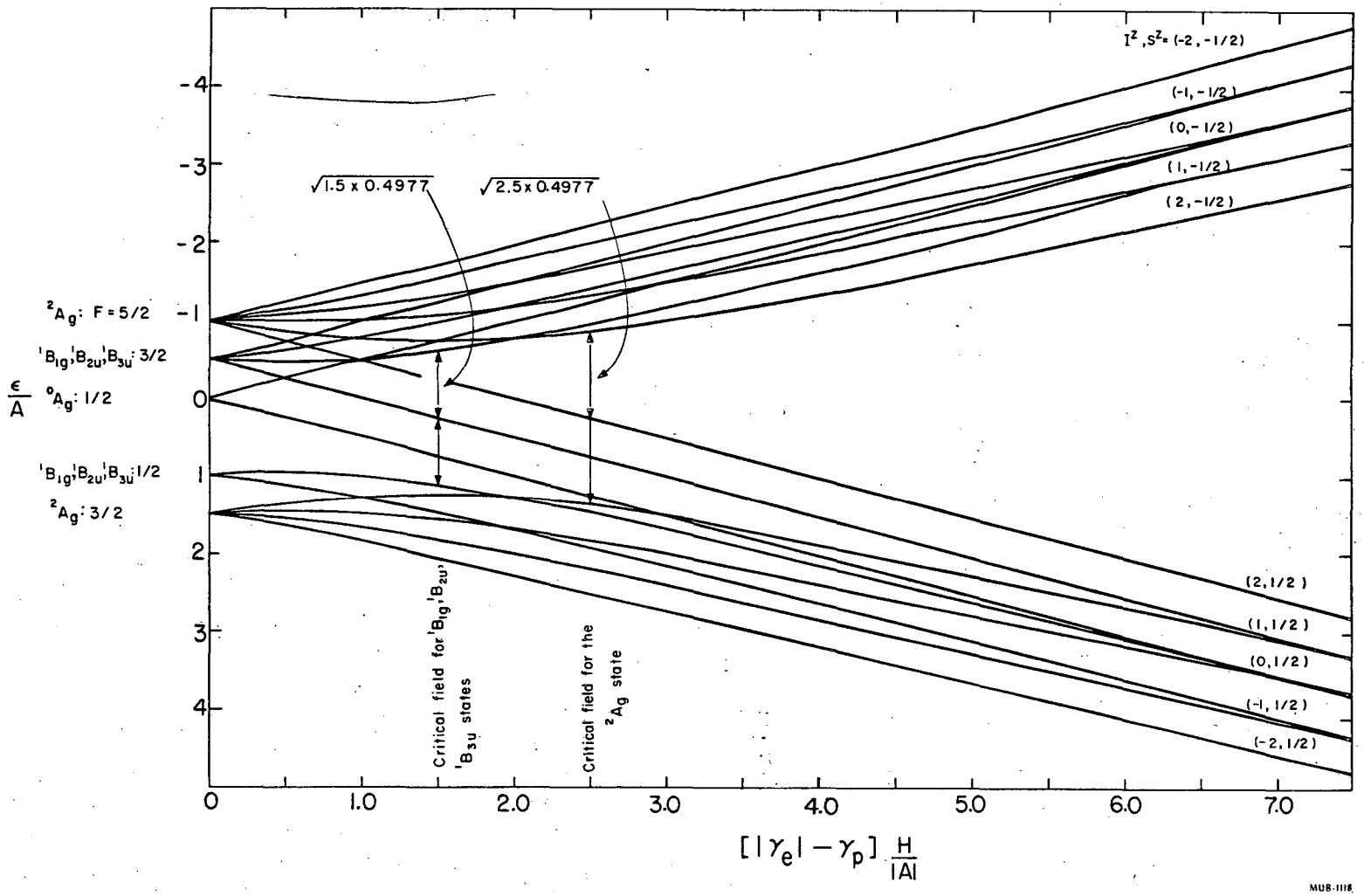
$I^2, S^z = (-2, -1/2)$
(-1, -1/2)
(0, -1/2)
(1, -1/2)
(2, -1/2)
$\sqrt{1.5 \times 0.4977}$
$\sqrt{2.5 \times 0.4977}$
^2A_g: F = 5/2
$^1B_{1g}, ^1B_{2u}, ^1B_{3u}$: 3/2
^0A_g: 1/2
$^1B_{1g}, ^1B_{2u}, ^1B_{3u}$: 1/2
^2A_g: 3/2
$\frac{\epsilon}{A}$
(2, 1/2)
(1, 1/2)
(0, 1/2)
(-1, 1/2)
(-2, 1/2)
Critical field for $^1B_{1g}, ^1B_{2u}, ^1B_{3u}$ states
Critical field for the ^2A_g state
$[|\gamma_e| - \gamma_p] \frac{H}{|A|}$
MUB-1118

Fig. 3

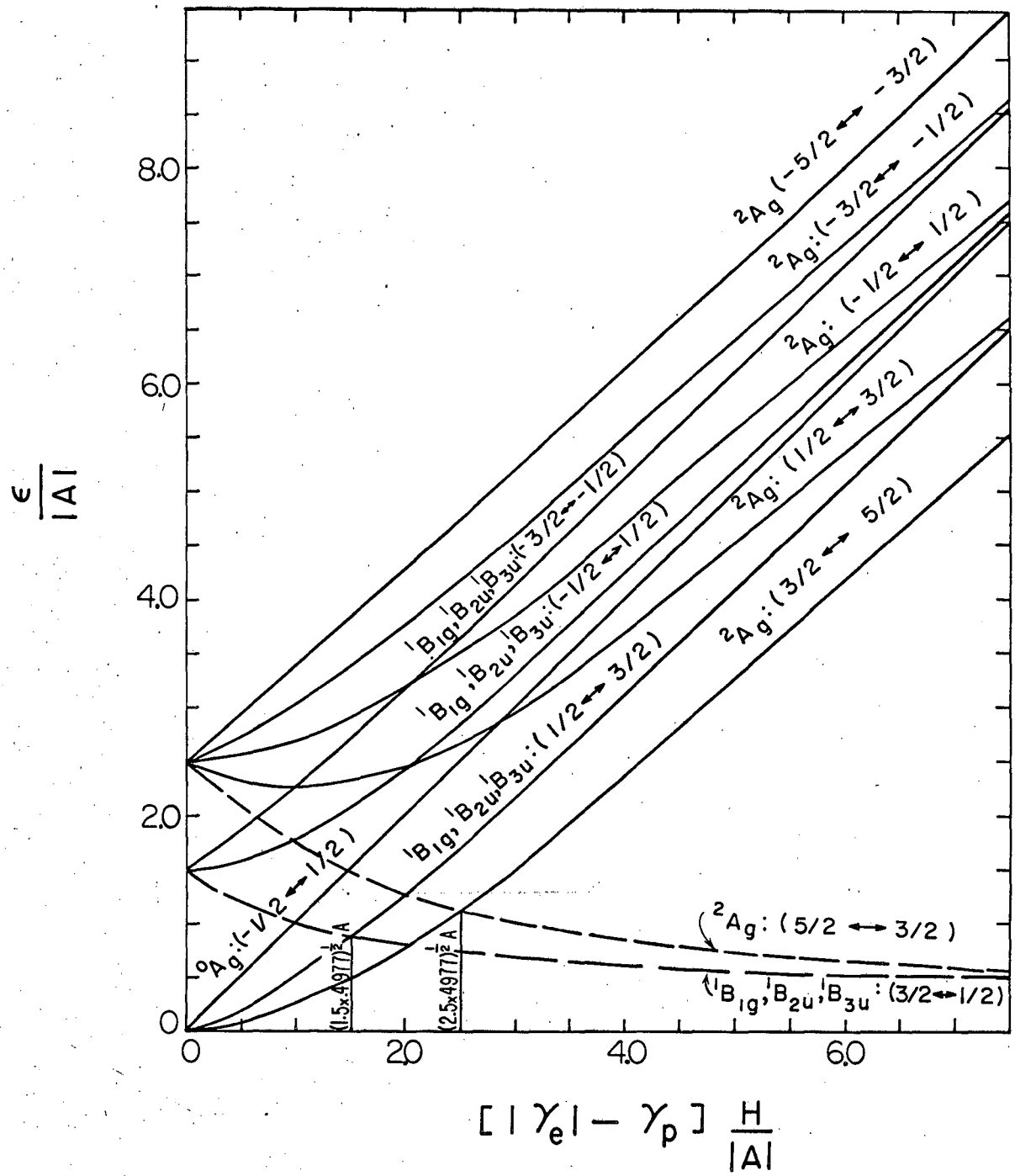

MUB-1114

Fig. 4

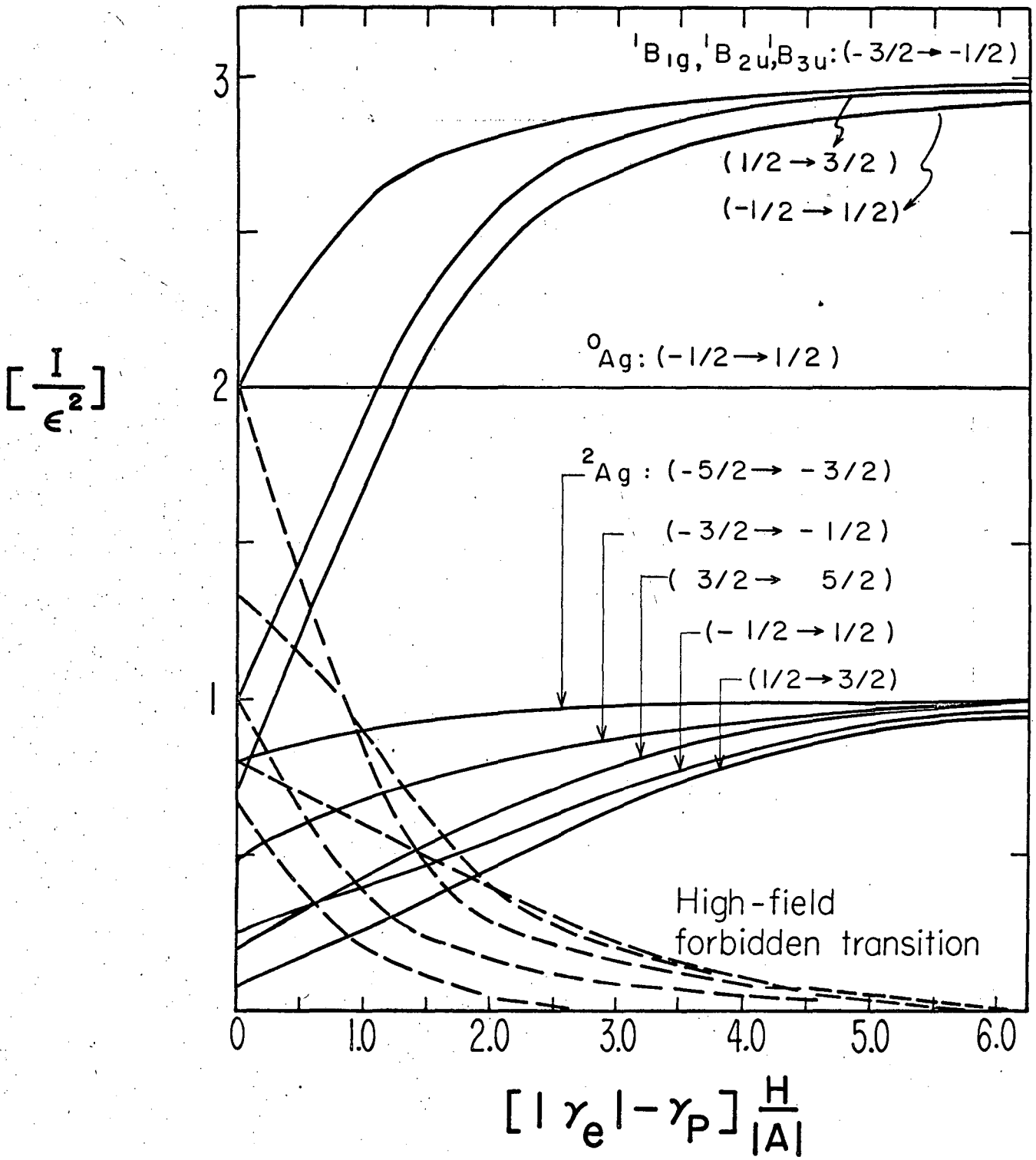

Fig. 5

MUB-1115